Mine Water and the Environment (2021) 40:497–509
https://doi.org/10.1007/s10230-021-00769-z

TECHNICAL ARTICLE

Prediction of Floor Failure Depth in Deep Coal Mines by Regression Analysis of the Multi-factor Influence Index

Yanbo Hu[1] · Wenping Li[2] · Shiliang Liu[3] · Qiqing Wang[2]

Received: 30 August 2019 / Accepted: 1 March 2021 / Published online: 8 March 2021

Abstract

A multivariate regression analysis model was developed to predict floor failure depth in deep mines using field measured data from 39 coal mining sites in the eastern mining area of the north China coalfields. A Brillouin optical time domain reflectometry system was built with distributed optical fiber sensors embedded in the floor of a coalface to measure the actual failure depth of the mine floor. The measured and predicted results were in good agreement. This study provides an effective scientific basis for preventing and controlling floor water inrush in deep mines in the north China coalfield.

Keywords Forecasting model · Hard rock coefficient · Thickness of aquiclude

Introduction

The eastern mining area of the north China coalfield has entered the deep mining stage, defined as exceeding 400 m below the surface. Deep seam mining is accompanied by complex conditions such as high geostress, high geotemperatures, and high karst water pressure. In recent years, the threat of Ordovician limestone karst water erupting from below the coal seam has become increasingly severe (Chen et al. 2018; Hu et al. 2019a; Hu 2020; Sun et al. 2016).

If the failure depth of a mine floor can be predicted effectively before mining takes place and a water inrush can be intercepted in time, floor water damage can be effectively avoided. In the 1930s, former Soviet scholar B. A. Slisalif put forward a formula to analytically calculate a safe aquiclude thickness for a coal seam floor (Liu 2014). Yugoslavian scholar Kuscer (1991) revealed the dynamic changes in hydrogeology during a water inrush, providing an important basis for prevention and control of water inrush from mining floors. In 1964, Chinese scholars proposed the concept of a water inrush coefficient, significantly contributing to the early warning of floor water inrushes (Liu 2009). Li et al. (1988) proposed the theory of the "down three zone." In the 1980s, the Xi'an Research Institute of the China Coal Research Institute proposed that the thickness of an effective floor aquiclude should not include the failure depth of the mine floor and revised the water inrush coefficient formula (Liu et al. 2018a). Wang (1988) deduced a calculation formula for the failure depth of mine floors using fracture mechanics. Ts-q and Ts-M methods (Qiao et al. 2009) were used to evaluate the risk of floor water inrush using the aquiclude thickness and water content of the floor aquifer (Sun et al. 2020).

In recent years, the mining depth of the eastern mining area has increased at a rate of 10–25 m per year, and the engineering geological conditions of deep mining have also undergone tremendous changes. Deep seam mining suffers from high crustal stress, high rock burst tendency, and high osmotic pressure. To effectively prevent and control water inrush from floors in deep mines, we focused our efforts on better predicting the failure depth of the mine floor. Using field measured data from 39 coal mining sites, we conducted multifactor regression modeling to forecast the floor failure depth in deep mines. A Brillouin optical time domain reflectometry system (BOTDRS) was built with distributed optical fiber sensors embedded in the floor of a coalface to measure the failure depth of the mining floor; the measured value was compared with the predicted value. This study provides

✉ Wenping Li
wplicumt@126.com

[1] School of Transportation Engineering, Nanjing Tech University, Nanjing 211816, Jiangsu, China

[2] School of Resources and Geosciences, China University of Mining and Technology, Xuzhou 221116, Jiangsu, China

[3] School of Civil and Engineering, Shandong University, Jinan 250061, Shandong, China

an effective scientific basis for improving prediction and control of floor water hazards in deep seam mining.

Study Area

The eastern mining area of the north China coalfield includes the Shandong mining area, the northern Jiangsu mining area, and the northern Anhui mining area (Fig. 1). Karst fissure

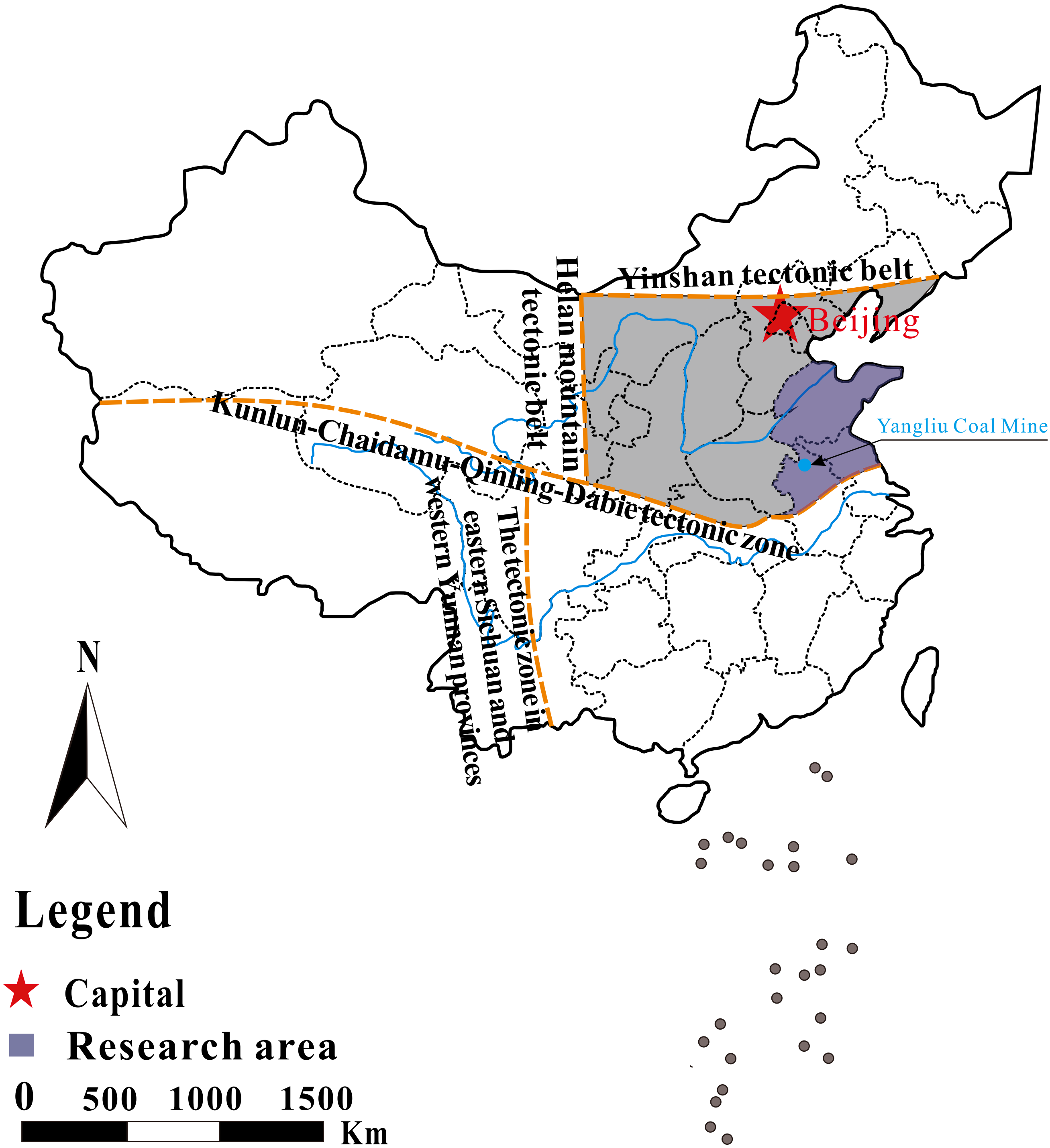

Fig. 1 Location of the research area

water in Permian, Carboniferous, and the Ordovician limestones all threaten the deep mines in this area. The mining of the lower coal group is severely threatened by inrush from the Ordovician limestone karst water. Ordovician limestone karst is dominated by dissolution fissures and cavities in which water is stored at high hydrostatic pressure.

Water movement in Ordovician limestone karst is largely controlled by bedding planes. Ordovician limestone is thick and pure in lithology; it is mainly composed of thick layered microcrystalline limestone with grey-yellow dolomitic limestone, lime dolomite, and thin mudstone with more stratification development (Li et al. 2019).

Water Inrush Mode of Floor Failure

The key factors for prediction and control of the water inrush from the floors in the lower-coal-group is the source and flow path of the water inrush. If the effective aquiclude thickness between the floor of the lower coal group and the top of limestone aquifer remains larger than the safe aquiclude thickness (the water inrush coefficient was calculated as 0.06 MPa/m), water inrush from the floor of the lower coal group can be predicted and controlled. The mine floor water inrush type can be categorized into three modes based on the effective aquiclude thickness of the seam floor. The first mode has the following conditions: (1) no fault is present; (2) the failure depth of the mine floor is relatively large; (3) the thickness of the effective aquiclude is less than is safe (Fig. 2). The second mode has the following conditions: (1) faults are present in the floor of coal seam; (2) the failure depth of the mine floor and faults form conduits for water inrush (Fig. 3). The third mode has the following conditions: (1) fractured zones are present in the coal seam floor; (2) the mining floor rock strata are collapsed; 3. The water-conducting cracks in the fractured zone extend into the stress release area behind the coal wall.

The water inflow mode changes from void flow to fissure flow and finally pipeline flow, leading to a delayed water inrush through the mine floor (Fig. 4). The three floor water

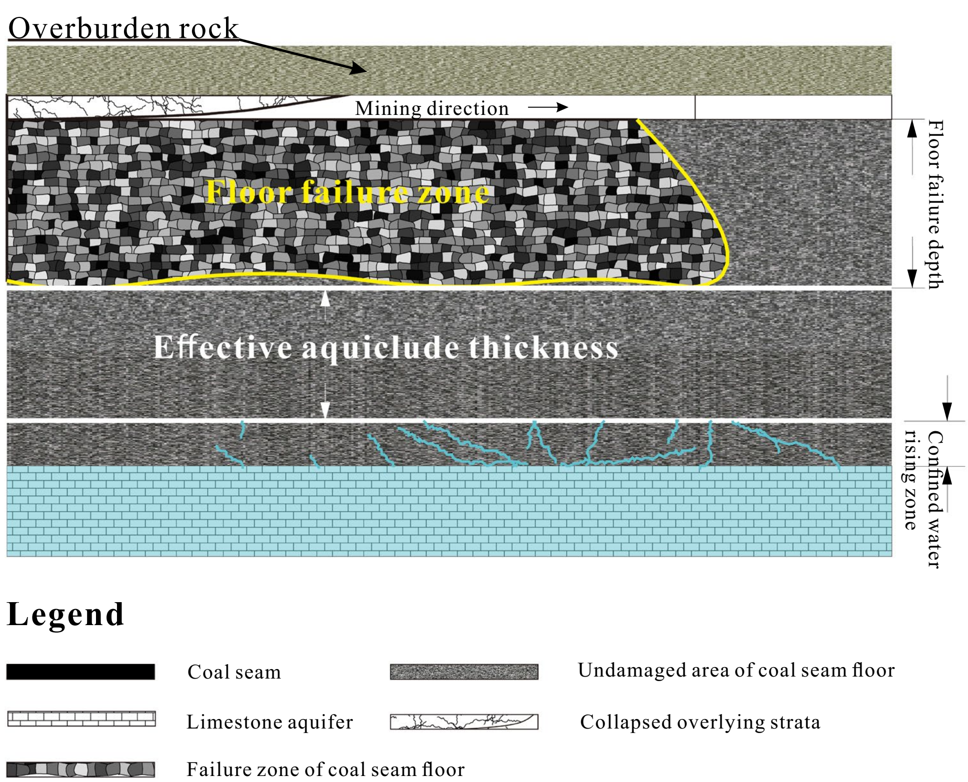

Fig. 2 Floor water inrush mode I in deep coal seam mining

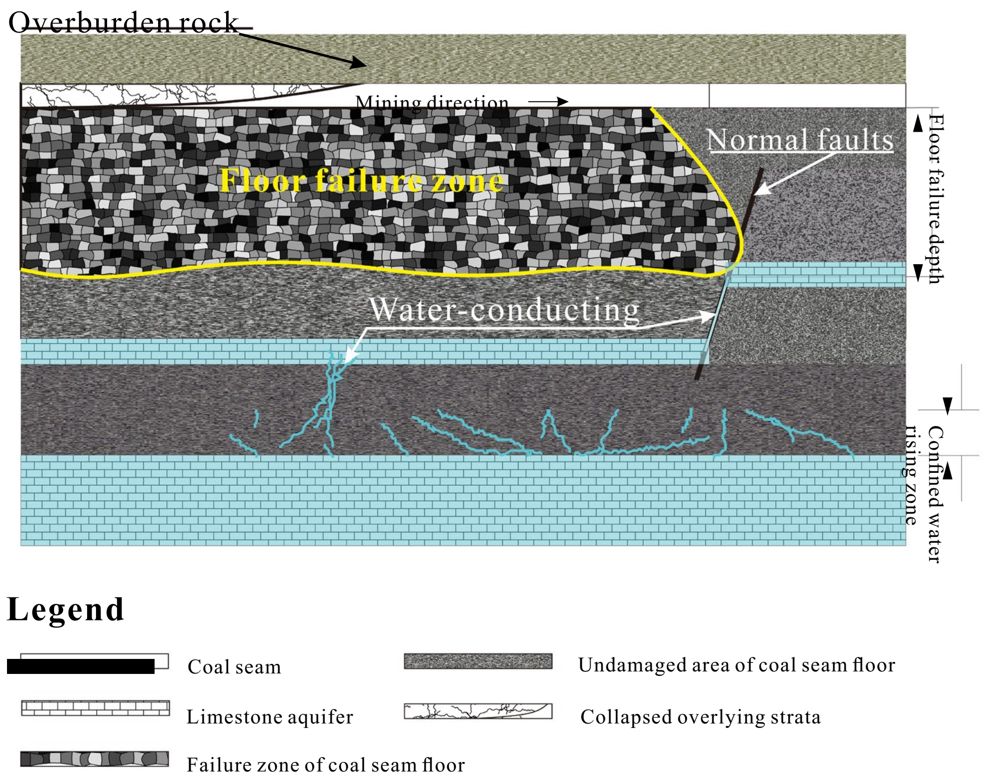

Fig. 3 Floor water inrush mode II in deep coal seam mining

inrush modes are all directly related to floor failure depth; thus, the depth of floor failure in deep coal seam mining directly affects the risk of floor water inrush. In this study, the floor failure depth of deep seam mining in the eastern mining area of the north China coalfields was evaluated.

Predicting Floor Failure Depth in Deep Mines

Analysis of Influencing Factors for Floor Rock Failure

According to the engineering geology and hydrogeology theory of coal mining and production practices in the eastern mining area of north China's coalfields, there are five factors that directly affect the floor failure depth of deep seam mining under normal conditions: coal seam depth (H), coal seam dip angle (α), mining thickness (M), coalface width (L), and the proportional coefficient of hard rock in the coal seam floor (β) (Chao et al. 2015; Hu et al. 2019d). Each factor is discussed in turn:

1. *Coal seam depth* According to the basic theory of coal geological engineering and rock mechanics, the size and direction of in-situ stress in rock strata near a deep excavation significantly affect the extent of damage to the surrounding rock (Chao et al. 2015; Jaeger and Cook 1979). The original rock stress of the surrounding rock in deep underground excavations increases with depth. Therefore, the depth of the coal seam is directly proportional to the depth of floor failure (Zhang et al. 2013).
2. *Coal seam dip angle* According to mechanical analysis of an inclined coal seam, the larger the dip angle of the coal seam, the larger the slip force (gravity component) of the roof during mining. The coal wall is affected by the gravity sliding force of the overlying strata. The concentrated stress of the coal wall increases, increasing the failure depth of the mine floor (Liu et al. 2018b).
3. *Coal seam mining thickness* An increase in mining coal seam thickness reduces the speed of mining, prolongs the stress release of floor rock in the goaf, allows the floor of goaf to fully expand, and increases the floor fail-

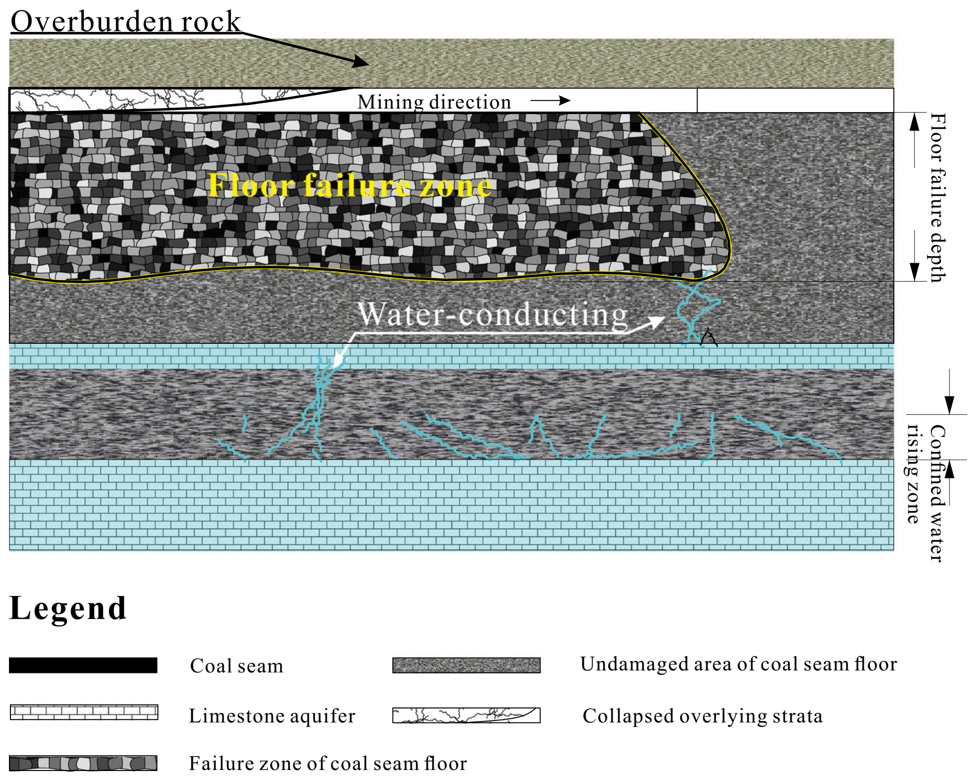

Fig. 4 Floor water inrush mode III in deep coal seam mining

ure depth. At the same time, according to the measured data, the floor failure depth is directly proportional to the mining thickness (Zhu et al. 2013).

4. *Coalface width* The failure depth of the mining floor is also closely related to the width of mining face. An increase in the inclined length of the mining face increases the area of roof control, which changes the pressure in the surrounding rock, thus affecting the failure depth (Zhang 2005).
5. *Hard rock coefficient of the mine floor* This refers to the failure mechanism of the floor in coal mining; the stress balance of the original rock is broken due to the excavation of the underground void. Using the cyclic process of mining technology in the coalface, the stresses in the surrounding rock is rebalanced. The breakage of floor rock is directly related to the surrounding rock pressure and ultimately the tensile strength of the floor rock. Therefore, a new index, the hard rock lithology ratio coefficient (β), is proposed. The proportional coefficient of a coal seam floor is calculated:

$$\beta = \frac{\sum h_n}{H/(30\tilde{3}5)}$$

where Σh_n is the cumulative thickness of hard rock strata within the estimated failure depth of the mine floor. The partial correlation coefficient of coal seam depth to mine floor failure depth is 0.70 (Table 1), indicating a close relationship between the two factors according to a partial correlation analysis of the mine floor failure depth. Therefore, according to the statistical analysis of measured data, the failure depth of the mine floor is generally ≈ 1/35–1/30 of the coal seam depth. So, the failure depth of deep coal seam mining floor is mainly related to these five factors.

Measured Floor Failure Zone Data

The existing empirical formula for floor failure depth does not satisfy the safety needs of deep seam mining (Hu et al. 2019a, b, c). In this study, information from 39 points were collected for the floor failure depth of north China mines

Table 1 Correlation analysis of various factors affecting the failure depth of the mine floor

	Independent variable	H (m)	α (°)	d (m)	L (m)	β (%)
Floor failure depth	Pearson correlation	0.701**	0.221	0.081	0.511**	0.708**
	Significant (bilateral)	0.000	0.051	0.480	0.000	0.000

**Significant correlation at 0.01 level (bilateral)

with depths > 400 m. Comprehensive analysis of floor failure depth was conducted based on measurements of various influencing factors.

Multivariate Regression Analysis of the Mine Floor Failure Depth

Multivariate regression analysis is a statistical analysis method where one variable is taken as a dependent variable and many other variables are taken as independent variables. This method establishes a quantitative relationship between linear or nonlinear mathematical models among multiple variables using sample data. A multivariate regression analysis method was developed to establish a forecasting model by analyzing the correlation between two or more independent variables and one dependent variable. When there is a linear relationship between independent and dependent variables, multiple linear regression analysis can be used. However, when many independent and dependent variables have a nonlinear relationship, the nonlinear model can be converted into a linear model to solve practical problems (Chung et al. 1995). The basic models of multivariate linear regression analysis are:

$$\mathrm{y} = \phi_0 + \phi_1 x_1 + \phi_2 x_2 + \cdots + \phi_n x_n \tag{1}$$

The regression coefficients are obtained using the least square method:

$$\mathrm{D} = \sum \left(y_i - \hat{y}_i\right) = \sum \left(y_i - \hat{\phi}_0 - \hat{\phi}_1 x_1 - \hat{\phi}_2 x_2 - \cdots - \hat{\phi}_n x_n\right)^2 = min. \tag{2}$$

D calculates the partial derivatives for $\hat{\phi}_0, \hat{\phi}_1, \hat{\phi}_2, \cdots \hat{\phi}_n$, respectively, making it equal to 0:

$$\begin{cases} \frac{\partial D}{\partial \hat{\phi}_0} = \sum \left(y_i - \hat{\phi}_0 - \hat{\phi}_1 x_1 - \hat{\phi}_2 x_2 - \cdots - \hat{\phi}_n x_n\right)(-1) = 0, \\ \frac{\partial D}{\partial \hat{\phi}_1} = \sum \left(y_i - \hat{\phi}_0 - \hat{\phi}_1 x_1 - \hat{\phi}_2 x_2 - \cdots - \hat{\phi}_n x_n\right)\left(-x_1\right) = 0, \\ \vdots \\ \frac{\partial D}{\partial \hat{\phi}_n} = \sum \left(y_i - \hat{\phi}_0 - \hat{\phi}_1 x_1 - \hat{\phi}_2 x_2 - \cdots - \hat{\phi}_n x_n\right)\left(-x_n\right) = 0. \end{cases} \tag{3}$$

The independent and dependent variables are known data; the estimated values $\hat{\phi}_0, \hat{\phi}_1, \hat{\phi}_2, \ldots \hat{\phi}_n$ of the parameters can be obtained by solving Eq. (3). The relationship between independent and dependent variables in regression equation can be established using Eq. (4):

$$R^2(y, 1, 2, \ldots, n) = \frac{\sum \left(\hat{y}_i - \bar{y}\right)^2}{\sum \left(y_i - \bar{y}\right)^2} \tag{4}$$

The closer that R^2 approaches 1, the more accurate the regression equation. In this study, SPSS software was used to achieve the regression analysis and predict various factors for the floor failure depth in deep coal seam mining. At the same time, the effects of coal seam depth, coal seam dip angle, mining thickness, coalface width, and hard rock coefficient of coal seam floor on the floor failure depth were evaluated.

A partial correlation analysis of various factors on the failure depth of deep mining floor was carried out using SPSS software, as shown in Table 1. To predict the accuracy of the multivariate regression equation, four factors with a larger Pearson correlation coefficient were selected for multivariate analysis to perform stepwise fitting analysis and prediction. The prediction equations were compared and analyzed, and the optimum fitting degree was selected.

Regression Analysis of Floor Failure Depth Considering L and β

A polynomial relationship between *L and β* and the floor failure depth was obtained by SPSS analysis and a three-dimensional relationship was obtained by fitting the data in Table 2 (Fig. 5). The two-factor fitting of floor failure model I is shown in Eq. 5.

$$h_1 = 1.237E - 5L^2 + 0.005L + 70.361\beta^2 - 59.665\beta + 18.883 \tag{5}$$

1. Prediction model II of floor failure depth in deep coal mining was obtained by considering three factors: the coal seam depth, coalface width, and hard rock coefficient of the mine floor. The fitting equation is:

$$h_2 = 0.014H + 0.789L^{0.436} + 0.056e^{6.282\beta} \tag{6}$$

2. Prediction model III was obtained by considering the same three factors along with the coal seam dip angle. The fitting equation is:

$$h_3 = 0.014H + 0.09\alpha + 0.453L^{0.516} + 0.068e^{6.062\beta} \tag{7}$$

Table 2 Measured values of the floor failure depth and related influencing factors

No.	Coalface	Coal seam depth (H(m))	Coal seam dip angle (α(°))	Mining thickness (M(m))	Coalface width (L(m))	Hard rock coefficient (β)	Failure depth (h(m))
1	Jingjing no. 1 mine (4707-1)	400.00	9	7.50	34	0.44	8.00
2	Jingjing no. 1 mine (4707-2)	400.00	9	4.00	34	0.41	6.00
3	Jingjing no. 1 mine (4707-3)	400.00	9	4.00	45	0.41	6.50
4	Feicheng F mine (9507)	400.00	7	1.30	120	0.81	20.40
5	Dongjiahe mine (22507)	408.00	7	3.00	114	0.49	10.80
6	Gaocheng mine (21021)	415.00	11	4.70	154	0.45	10.00
7	Guoning no. 1 mine (213)	416.00	18	1.50	115	0.69	16.50
8	Caozhuang mine (8812-1)	420.00	20	2.00	120	0.85	18.50
9	Qiuji mine (1102)	428.63	8	2.02	60	0.69	16.00
10	Chaohua mine (22121)	430.00	17	10.00	101	0.59	15.00
11	Caozhuang mine (8812-2)	442.00	20	2.00	125	0.93	36.50
12	Liuqiao no. 1 mine (III423)	450.00	9	1.90	170	0.79	21.00
13	Suntong mine (1028)	466.00	17	3.40	180	0.59	17.00
14	Xinglong mine (10302)	467.00	7	8.90	200	0.84	19.00
15	Feicheng H mine (8203)	468.00	7	1.90	85	0.91	27.40
16	Linyi D mine	470.00	15	4.00	120	0.21	13.00
17	Qingdong mine (104)	489.00	15	2.80	321	0.35	16.90
18	Taoyuan mine (1066)	500.00	28	3.40	112	0.45	16.00
19	Liuqiao no. 2 mine (2614)	500.00	9	2.90	160	0.21	14.90
20	Huafeng mine (41303)	520.00	30	0.90	120	0.51	13.00
21	Baizhuang mine (7105)	520.00	10	1.50	80	0.81	21.60
22	Yangmie no. 5 mine (8403)	520.00	9	8.80	220	0.75	20.00
23	Zhaogu no. 1 mine (11111)	570.00	2	3.50	175	0.68	23.50
24	Chensilou mine (21301)	584.00	10	2.70	149	0.51	14.00
25	Pansan mine (37-1)	590.00	15	3.00	205	0.61	14.60
26	Dongtan mine (1305)	598.00	6	8.80	223	0.81	20.00
27	Qianyingzhi mine (13)	630.00	9	3.50	200	0.43	17.00
28	Liangzhuang mine (51302-1)	640.00	12	1.00	165	0.84	35.00
29	Liangzhuang mine(51101W)	640.00	15	1.50	165	0.81	20.10
30	Xinji no. 2 mine	650.00	10	4.50	150	0.75	19.20
31	Qianyingzhi mine (12)	650.00	9	3.50	150	0.78	24.30
32	Zhaogu no. 1 mine (11011)	710.00	3	3.60	180	0.76	25.80
33	Huafeng mine (2-41303)	721.00	30	0.90	120	0.61	12.00
34	Zhaogezhuang mine (1237-1)	900.00	26	2.00	200	0.83	27.00
35	Zhaolou mine (1304-2)	985.00	4	4.80	205	0.75	22.60
36	Zhaogezhuang mine(12370-2)	1000.00	30	2.00	200	0.82	38.00
37	Xingdong mine (2121)	1000.00	12	3.70	150	0.69	32.50
38	Hanxing region T mine (1212)	1000.00	10	3.50	150	0.72	33.80
39	Zhaogezhaung mine (1237)	1056.00	26	10.00	200	0.78	35.00

Zhang (2016), Zhang and Chang (2018)

where h_x is the forecasted failure depth of mining floor; H is the depth of coal seam; α is the coal seam dip angle; L is the width of coalface; β is the hard rock coefficient of coal seam floor.

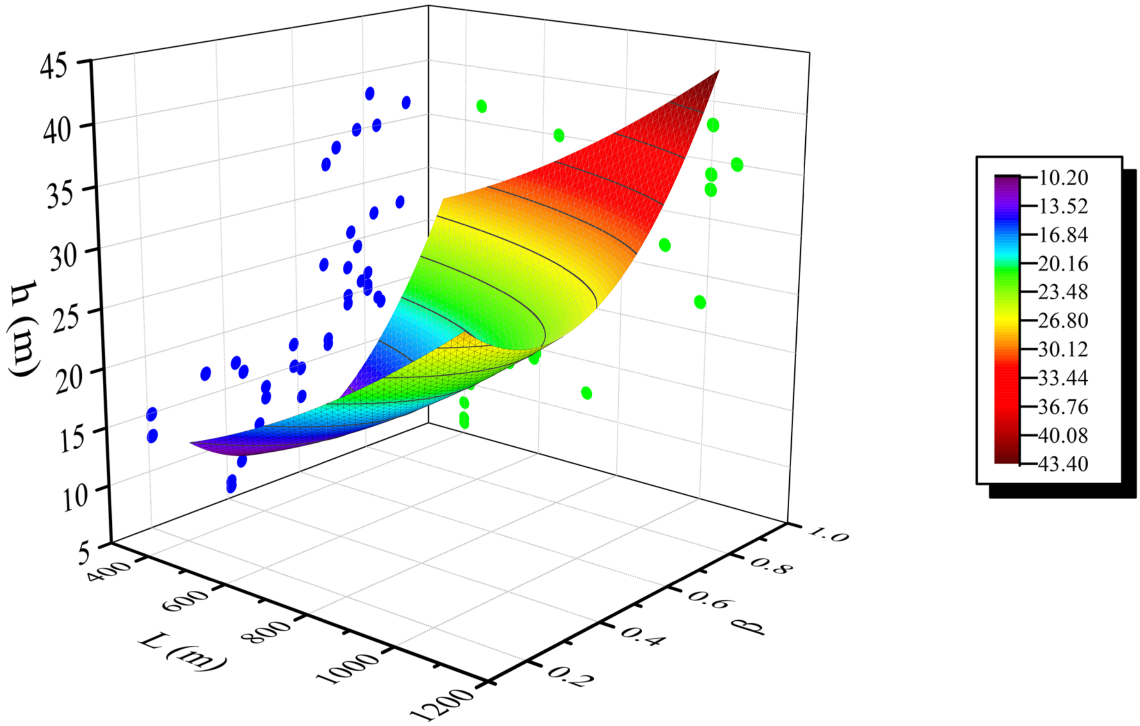

Fig. 5 Fitting graph of two independent variables and one dependent variable

Results and Discussion

Accuracy of Mine Floor Failure Depth Forecasts by Contrastive Analysis

Based on the three models for forecasting the floor failure depth obtained in this study, the empirical formulas for the eastern mining area of North China-type coalfields were compared and analyzed (Table 3). An empirical prediction of floor failure depth is shown in Eq. (8) (Kang and Liu 2011):

$$h = 0.0085H + 0.1665\alpha + 0.1079L - 4.3579$$

As shown in Table 3, the traditional empirical formula is no longer applicable to predicting floor failure depth in deep mines. According to the relative error data of multifactor regression, the predictive error of floor failure depth in deep mines under normal conditions was the least when four factors were considered: the coal seam depth and dip angle, the width of the coalface, and the hard rock coefficient of the mine floor. Therefore, multifactor regression analysis prediction model III provides the best solution.

Field Test Results

The floor failure depth of the Yangliu coal mine 10-H mining face in the eastern mining area of the north China coalfield was predicted using multivariate regression prediction model III. The predicted results were verified by the BOTDRS-measured floor failure depth.

Predicted Floor Failure Depth

The Yangliu coal mine 107 mining area 10-H coalface has the following characteristic: surface elevation + 25 m, coalface elevation −451.2 m, coalface length 1119.4 m, coalface width 166.2 m, coal seam dip angle 7°, and coal seam thickness 3.2 m. According to experience of mining the no. 10 coal in the Huaibei mining area, the failure depth of the mine floor is between 1/35–1/30 of the coal seam depth under normal conditions (the floor does not contain faults). Therefore, when calculating the hard rock ratio coefficient (β), the rock strata within 20 m of the coal seam floor is included. As shown in Fig. 6, $\beta = 18.4/20 = 0.92$.

The predicted floor failure depth of the 10-H coalface using model III was calculated by:

$$h_3 = 0.014H + 0.09\alpha + 0.453L^{0.516} + 0.068e^{6.062\beta} \approx 17.35\ \text{m}$$

Table 3 Error data between forecasted and measured failure depth of the mine floor

No	Coalface	Failure depth (m)	Empirical formula		Model I		Model II		Model III	
			Predictive value	Relative error	Predictive value	Relative error	Predictive value	Relative error	Predictive value	Relative error
1	Feicheng F coal mine (9507)	20.40	13.16	−0.36	17.50	−0.14	21.04	0.03	20.81	0.02
2	Qiuji coal mine (1102)	16.00	7.09	−0.56	11.56	−0.28	14.98	−0.06	14.92	−0.07
3	Chaohua coal mine (22121)	15.00	13.03	−0.13	8.80	−0.41	14.20	−0.05	14.88	−0.01
4	Caozhuang coal mine (8812-2)	36.50	16.22	−0.56	25.07	−0.31	31.96	−0.12	32.55	−0.11
5	Liuqiao no. 1 coal mine (III423)	21.00	19.31	−0.08	16.87	−0.20	21.71	0.03	21.69	0.03
6	Suntong coal mine (1028)	17.00	21.86	0.29	9.47	−0.44	16.40	−0.04	17.09	0.01
7	Feicheng H coal mine (8203)	27.40	9.96	−0.64	23.37	−0.15	29.04	0.06	28.58	0.04
8	Linyi D coal mine	13.00	15.08	0.16	10.23	−0.21	13.15	0.01	13.53	0.04
9	Qingdong coal mine (104)	16.90	36.93	1.19	9.50	−0.44	17.12	0.01	17.66	0.05
10	Liuqiao no. 2 coal mine (2614)	14.90	18.65	0.25	10.57	−0.29	14.42	−0.03	14.27	−0.04
11	Baizhuang coal mine (7105)	21.60	10.36	−0.52	17.20	−0.20	21.69	0.01	21.75	0.01
12	Qianyingzhi coal mine (13)	17.00	24.08	0.42	7.73	−0.55	17.60	0.04	17.52	0.03
13	Qianyingzhi coal mine (12)	24.30	18.85	−0.22	16.18	−0.33	23.63	−0.03	23.61	−0.03
14	Zhaogezhuang coal mine (12370)	38.00	30.72	−0.19	18.76	−0.51	31.62	−0.17	33.48	−0.12
15	Hanxing region T coal mine (1212)	33.80	21.99	−0.35	13.43	−0.60	26.17	−0.23	26.26	−0.22
16	Zhaogezhaung coal mine (1237)	35.00	30.53	−0.13	16.65	−0.52	30.25	−0.14	31.79	−0.09

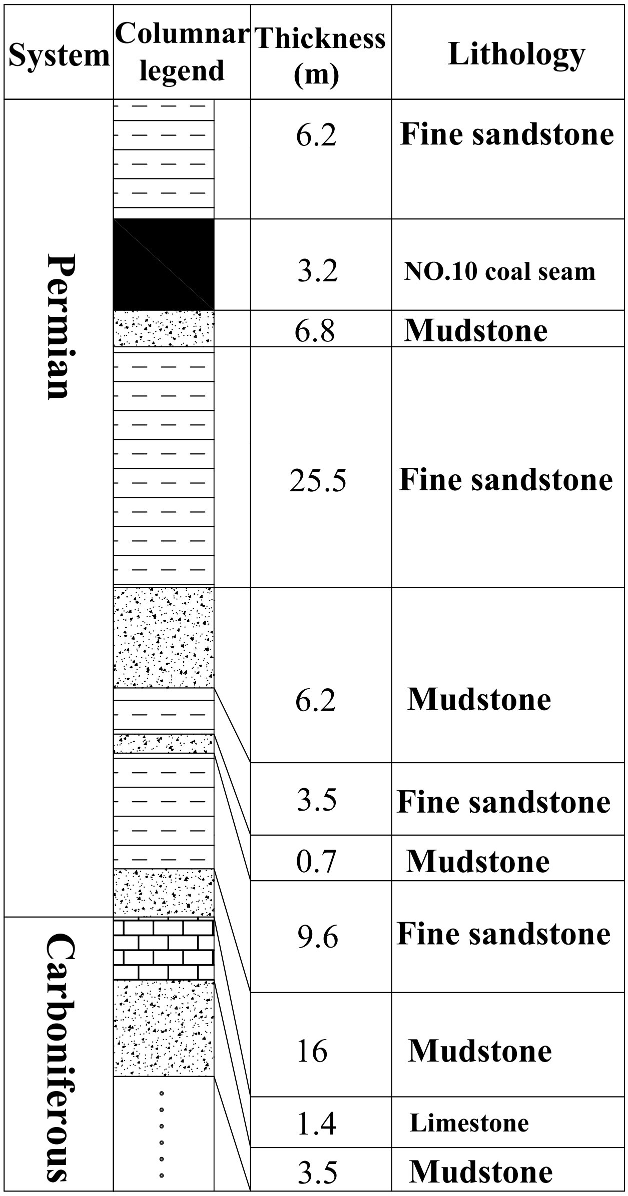

Fig. 6 Stratigraphy column of the 10-H mining face in research area

Measuring the Failure Depth of the Mine Floor by Distributed Optical Fiber

Optical fiber sensors were embedded in the floor of a coal mining face in the study area, and a BOTDRS was established by connecting an optical fiber strain distribution tester. The Brillouin scattered light was generated in the opposite direction of the incident light by the interaction between the light injected into the fiber and the crystal structure of medium in the conventional G. 652 single-mode fiber at 1550 nm detection wavelength. The Brillouin scattered light fluctuated regularly when the strain or temperature of the propagating medium changed (Fig. 7), showing that the Brillouin frequency shift of optical fibers is linearly related to the strain (Gu et al. 2018).

A gas pumping-exhaust tunnel is present at a depth of 40 m under the no. 10 coal seam floor. A borehole with a diameter of 91 mm was constructed from the roof of the gas pumping-exhaust tunnel at a 45° angle to the floor of coalface. Distributed optical fiber sensors were embedded before the mining. According to the properties of rock strata through which the borehole passes, layered grouting was carried out to achieve a synchronous strain among the sensors, fillers, and the rock surrounding the drill holes (Fig. 8) (Liu et al. 2018b).

During the mining of the 10-H mine face, the strain of the floor rock strata was monitored every 24 h. The breaking critical values (field sampling, laboratory test data) of the limit strain of rock strata at the corresponding locations were compared using the strain data of each 0.05 m, as measured by the distributed sensing optical fibers. If the monitoring strain exceeds the limiting value of rock strain breakage, it can be concluded that the rock stratum is breaking or broken.

The BOTDRS results are shown in Fig. 9. The failure depth of the floor near the coal wall reached a maximum of 16.67 m (b line). Line a shows the initial breaking position of the mine floor. Line c shows the maximum strain development of the mine floor strata. After line c, the mine floor was affected by roof collapse and the strain of floor rock gradually decreased, then recovered.

Contrastive Analysis of Predicted and Measured Values

The relative error between the predicted and measured values of multivariate regression prediction model III was 4%, indicating that the predicted result of model III was consistent with the actual situation and provides a scientific basis for the prediction and control of floor water hazard in deep mining for this mine (Table 4).

Conclusion

The failure depth of the coal seam floor is an important index of assessing the risk of mine floor water hazards. This study improved the accuracy of floor water hazard risk assessment and provides an important reference value for early warning of a water hazard for deep mines.

1. The hard rock coefficient of the mine floor is a new index that affects the failure depth of deep mining floor. It reflects the combined structure of both the soft and hard rock strata of the mining floor. The results show that this hard rock coefficient is closely related to the failure depth of the mine floor.

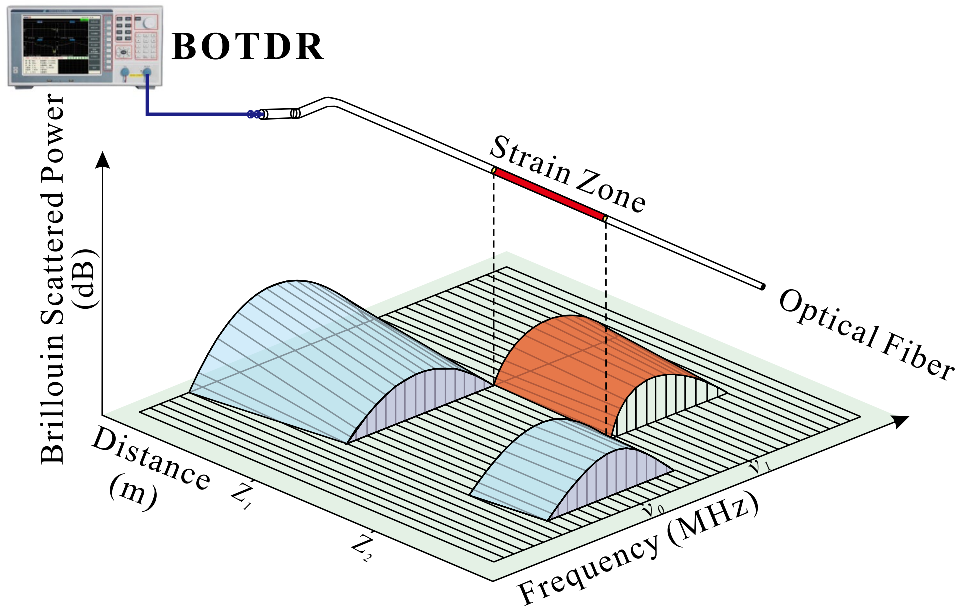

Fig. 7 Principle of BOTDRS

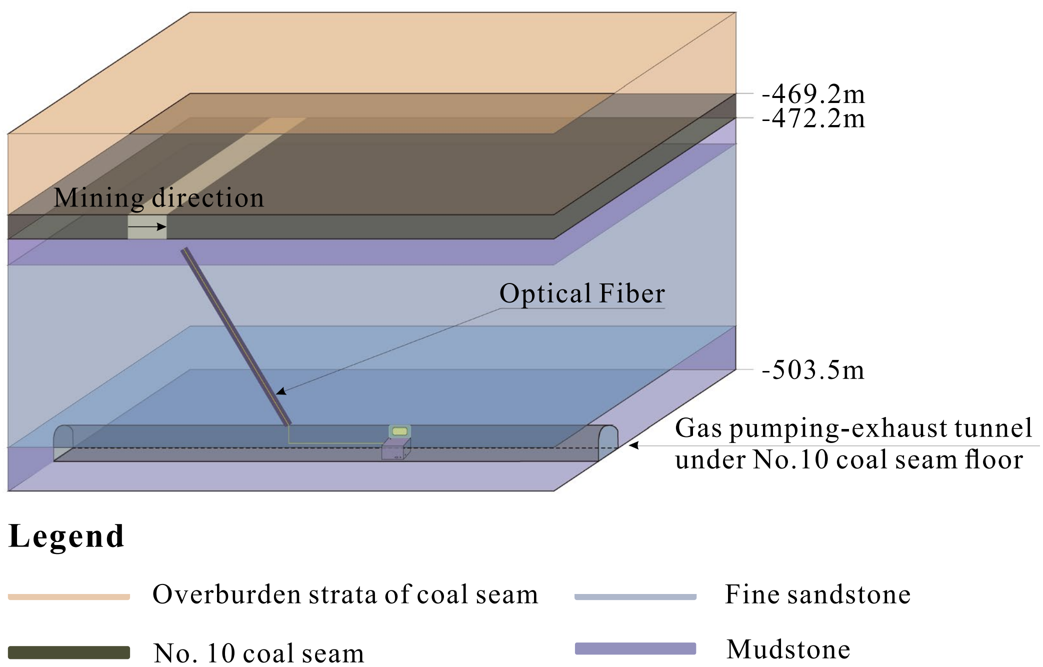

Fig. 8 Distributed optical fiber monitoring diagram of the 10-H mine face floor

2. Based on a case study of 39 points from the north China coalfields and regression analysis of a combination model of different independent and dependent variables, three nonlinear prediction models were obtained for the failure depth of the coal seam floor in a deep mine.
3. Three prediction models and empirical prediction formulas for floor failure depth in deep mining were compared. The results showed a small relative error between model III predicted values and the measured values.

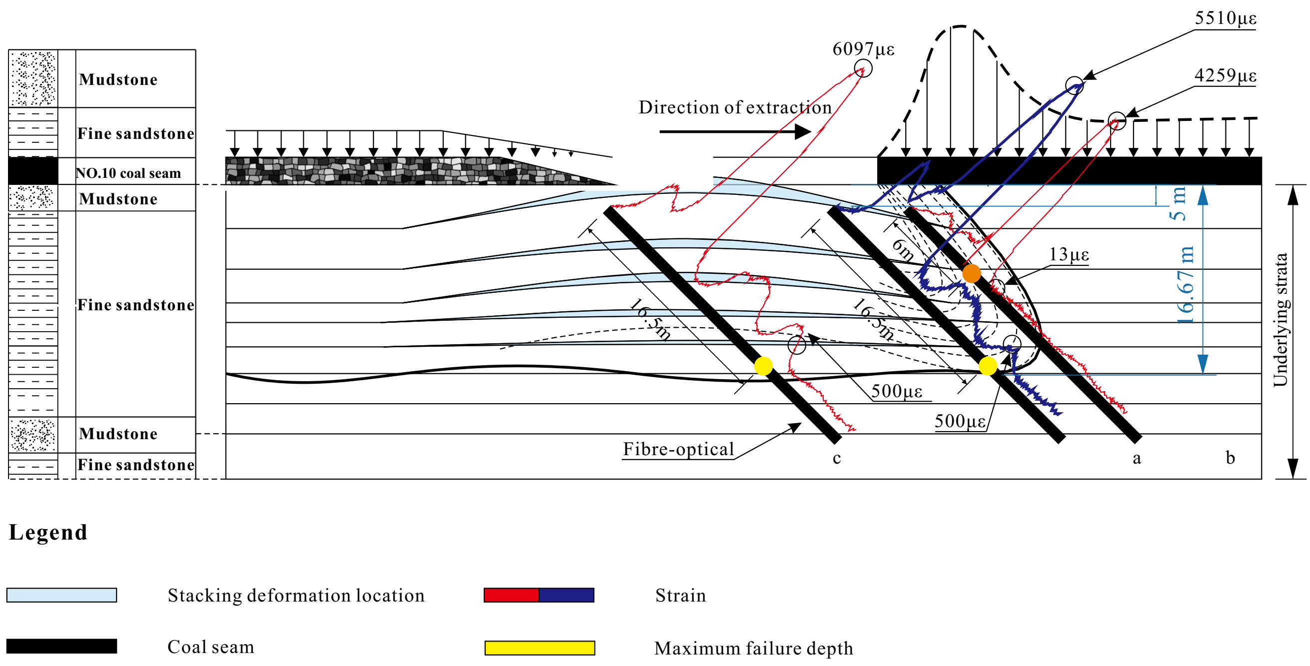

Fig. 9 Monitoring results of BOTDRS in the floor of the 10-H coalface in the study area

Table 4 Prediction and measurement data of floor failure depth of the 10-H coalface in the study area for Model III

Failure depth (h/m)	Predictive value	Relative error
16.67	17.35	0.04

4. Using model III to predict the floor failure depth of the 10-H coalface in the Yangliu coal mine, the accuracy of the predictions was relatively high. This study provides a scientific basis for the prediction and control of floor water hazards in deep mines in the eastern mining area of north China.

Acknowledgements This work was supported by the National Basic Research Program of China (973 Program) under Grant 2015CB251601, the State Key Program of the National Natural Science Foundation of China under Grant 41430643, and the Fundamental Research Funds for the Central Universities under Grant 2017XKZD07.

References

Chao WG, Liu XM, Zhang YJ (2015) Engineering geology. Hunan University Press, Changsha (**in Chinese**)

Chen L, Feng X, Xu D, Zeng W, Zheng Z (2018) Prediction of water inrush areas under an unconsolidated, confined aquifer: the application of multi-information superposition Based on GIS and AHP in the Qidong coal mine, China. Mine Water Environ 37(4):786–795. https://doi.org/10.1007/s10230-018-0541-1

Chung CJF, Fabbri AG, Van Westen CJ (1995) Multivariate regression analysis for landslide hazard zonation. Adv Nat Technol Haz. https://doi.org/10.1007/978-94-015-8404-3_7

Gu K, Shi B, Liu C, Jiang H, Li T, Wu J (2018) Investigation of land subsidence with the combination of distributed fiber optic sensing techniques and microstructure analysis of soils. Eng Geol 240:34–47. https://doi.org/10.1016/j.enggeo.2018.04.004

Hu YB (2020) Dynamic evolution law of fracture distribution and water inrush risk assessment in deep mining coal seam floor. Diss, China Univ of Mining and Technology. https://doi.org/10.27623/d.cnki.gzkyu.2020.000543

Hu YB, Li WP, Liu SL, Wang QQ, Wang ZK (2019a) Risk assessment of water inrush from aquifers underlying the Qiuji coal mine in China. Arab J Geosci 12(3):98. https://doi.org/10.1007/s12517-019-4244-0

Hu YB, Li WP, Wang QQ, Liu SL, Wang ZK (2019b) Evolution of floor water inrush from a structural fractured zone with confined water. Mine Water Environ 38(2):252–260. https://doi.org/10.1007/s10230-019-00599-0

Hu YB, Li WP, Wang QQ, Liu SL, Wang ZK (2019c) Evaluation of water inrush risk from coal seam floors with an AHP–EWM algorithm and GIS. Environ Earth Sci 78(10):290. https://doi.org/10.1007/s12665-019-8301-5

Hu YB, Li WP, Wang QQ, Liu SL, Wang ZK (2019d) Study on failure depth of coal seam floor in deep mining. Environ Earth Sci. https://doi.org/10.1007/s12665-019-8731-0

Jaeger JC, Cook NGW (1979) Fundamentals of rock mechanics, 3rd edn. Science Paperbacks, vol 9, no 3, pp 251–252. https://doi.org/10.1111/j.1468-8123.2009.00251.x

Kang YM, Liu CW (2011) Study on the strength of protective coal pillar in coal mining under building, railway and water and theory of new support technology. Met Mine 9:25–27 (**in Chinese**)

Kuscer D (1991) Hydrological regime of the water inrush into the Kotredez coal mine (Slovenia, Yugoslavia). Mine Water Environ 10(1):93–101

Li BY, Sheng GH, Jing ZG, Gao H (1988) Theory and practice of preventing water inrush from floor of mining face. Saf Coal Mines 5:47–48 (**in Chinese**)

Li Y, Xu J, Tao Z (2019) Analysis of water conductivity and water gushing source of collapse column in Changcun mine. Earth Environ Sci 267(5):052–061

Liu QS (2009) A discussion on water inrush coefficient. Coal Geol Explor 37(4):34–37. https://doi.org/10.3969/j.issn.1001-1986.2009.04.009

Liu HH (2014) Fundamental concept of indication layer in coal floor mining under water pressure. China Univ of Mining and Technology Press, Xuzhou, pp 59–63

Liu W, Mu D, Xie X, Yang L, Wang D (2018a) Sensitivity analysis of the main factors controlling floor failure depth and a risk evaluation of floor water inrush for an inclined coal seam. Mine Water Environ 37(3):636–648. https://doi.org/10.1007/s10230-017-0497-6

Liu Y, Li W, He J, Liu S, Cai L, Cheng G (2018b) Application of Brillouin optical time domain reflectometry to dynamic monitoring of overburden deformation and failure caused by underground mining. Int J Rock Mech Min Sci 106:133–143. https://doi.org/10.1016/j.ijrmms.2018.04.030

Qiao W, Li WP, Zhao CX (2009) Water inrush coefficient-unit inflow method for water inrush evaluation of coal mine floor. Chin J Rock Mech Eng 28(12):2466–2474. https://doi.org/10.3321/j.issn:1000-6915.2009.12.012 (**in Chinese**)

Sun W, Zhou W, Jiao J (2016) Hydrogeological classification and water inrush accidents in China's coal mines. Mine Water Environ 35(2):214–220. https://doi.org/10.1007/s10230-015-0363-3

Sun W, Zhou F, Liu J, Shao J (2020) Experimental study on Portland cement/calcium sulfoaluminate binder of paste filling. Eur J Environ Civ Eng. https://doi.org/10.1080/19648189.2020.17317122020.17317122020.17317122020.1731712

Wang (1988) Zero position failure theory of coal seam floor rock mass movement. Hebei Coal 04:36–39 (**in Chinese**)

Zhang JC (2005) Investigations of water inrushes from aquifers under coal seams. Int J Rock Mech Min Sci 42(3):350–360. https://doi.org/10.1016/j.ijrmms.2004.11.010

Zhang FD (2016) Study on deformation failure mechanism of deep coal seam floor and evaluation method of water inrush mining above confined aquifer. Diss, China Univ of Mining and Technology

Zhang B, Chang XF (2018) Prediction method and application of coal mining floor failure depth. Coal Technol 37(12):20–23. https://doi.org/10.13301/j.cnki.ct.2018.12.008

Zhang R, Jiang ZQ, Li XH, Chao HD, Sun J (2013) Study on the failure depth of thick seam floor in deep mining. J China Coal Soc 38(1):67–72. https://doi.org/10.13225/j.cnki.jccs.2013.01.024

Zhu SY, Jiang ZQ, Cao DT, Sun Q, Yang CW (2013) Restriction function of lithology and its composite structure to deformation and failure of mining coal seam floor. Nat Hazards 68(2):483–495. https://doi.org/10.1007/s11069-013-0623-0